

# Single-molecule imaging reveals mechanisms of protein disruption by a DNA translocase

Ilya J. Finkelstein<sup>2</sup>, Mari-Liis Visnapuu<sup>2</sup> & Eric C. Greene<sup>1,2</sup>

In physiological settings, nucleic-acid translocases must act on substrates occupied by other proteins, and an increasingly appreciated role of translocases is to catalyse protein displacement from RNA and DNA<sup>1–4</sup>. However, little is known regarding the inevitable collisions that must occur, and the fate of protein obstacles and the mechanisms by which they are evicted from DNA remain unexplored. Here we sought to establish the mechanistic basis for protein displacement from DNA using RecBCD as a model system. Using nanofabricated curtains of DNA and multicolour single-molecule microscopy, we visualized collisions between a model translocase and different DNA-bound proteins in real time. We show that the DNA translocase RecBCD can disrupt core RNA polymerase, holoenzymes, stalled elongation complexes and transcribing RNA polymerases in either head-to-head or head-to-tail orientations, as well as EcoRI<sup>E111Q</sup>, lac repressor and even nucleosomes. RecBCD did not pause during collisions and often pushed proteins thousands of base pairs before evicting them from DNA. We conclude that RecBCD overwhelms obstacles through direct transduction of chemomechanical force with no need for specific protein–protein interactions, and that proteins can be removed from DNA through active disruption mechanisms that act on a transition state intermediate as they are pushed from one non-specific site to the next.

RecBCD is a heterotrimeric translocase involved in initiating homologous recombination and processing stalled replication forks<sup>5,6</sup>. RecB is a 3' → 5' SF1A helicase and contains a nuclease domain for DNA processing, RecD is a 5' → 3' SF1B helicase and RecC holds the complex together and coordinates the response to *cis*-acting Chi (crossover hot-spot instigator) sequences (5'-dGCTGGTGG-3'). RecD is the lead motor before Chi, RecB is the lead motor after Chi and Chi recognition is accompanied by a reduced rate of translocation corresponding to the slower velocity of RecB<sup>7,8</sup>. Chi prompts RecBCD to process DNA, yielding 3' single-stranded DNA overhangs onto which RecA is loaded<sup>7,8</sup>.

We monitored RecBCD activity using total-internal-reflection fluorescence microscopy and a DNA curtain assay that allows us to visualize hundreds of aligned molecules<sup>9</sup> (Supplementary Fig. 1). When assayed on DNA curtains, RecBCD displayed rapid translocation ( $1,484 \pm 167$  base pairs per second ( $\text{bp s}^{-1}$ ), 37 °C, 1 mM ATP,  $N = 100$ ; Supplementary Fig. 1b, c), high processivity ( $36,000 \pm 12,500$  bp) and decreased velocity in response to Chi ( $549 \pm 155 \text{ bp s}^{-1}$ , 37 °C, 1 mM ATP,  $N = 100$ ; Supplementary Fig. 1), in agreement with previous studies<sup>6,7</sup>.

*Escherichia coli* contains ~2,000 molecules of RNA polymerase (RNAP), and ≥65% of these are bound to the bacterial chromosome<sup>10</sup>, making RNAP one of the most commonly encountered obstacles in physiological settings. RNAP is of special interest because it is a high-affinity DNA-binding protein (dissociation constant,  $K_d \approx 10 \text{ pM}$  for  $\lambda P_R$  and 100 pM for  $\lambda P_L$ ) and a powerful translocase capable of moving under an applied load of ~14–25 pN (ref. 11). RNAP survives encounters with replication forks<sup>12–14</sup> and stalls fork progression in head-on collisions<sup>15,16</sup>, suggesting that RNAP is among the most formidable roadblocks encountered *in vivo*. During replication restart, RecBCD translocates towards *oriC*; therefore, most collisions with

RNAP will occur in a head-on orientation, suggesting that to survive these encounters RecBCD would need to exert more force than a replisome.

We used quantum dots (QDs) to fluorescently label RNAP (Supplementary Information). The binding distribution of QD–RNAP holoenzyme overlapped with known promoters (Fig. 1a), promoter targeting was  $\sigma^{70}$  dependent and promoter-bound holoenzymes were highly stable ( $t_{1/2} = 23.2 \pm 1.42 \text{ min}$  (half-life),  $N = 58$ ; Supplementary Fig. 3a, b, c). Core QD–RNAP dissociated when challenged with heparin ( $t_{1/2} = 3.4 \pm 0.03 \text{ s}$ ,  $N = 150$ ), whereas promoter-bound

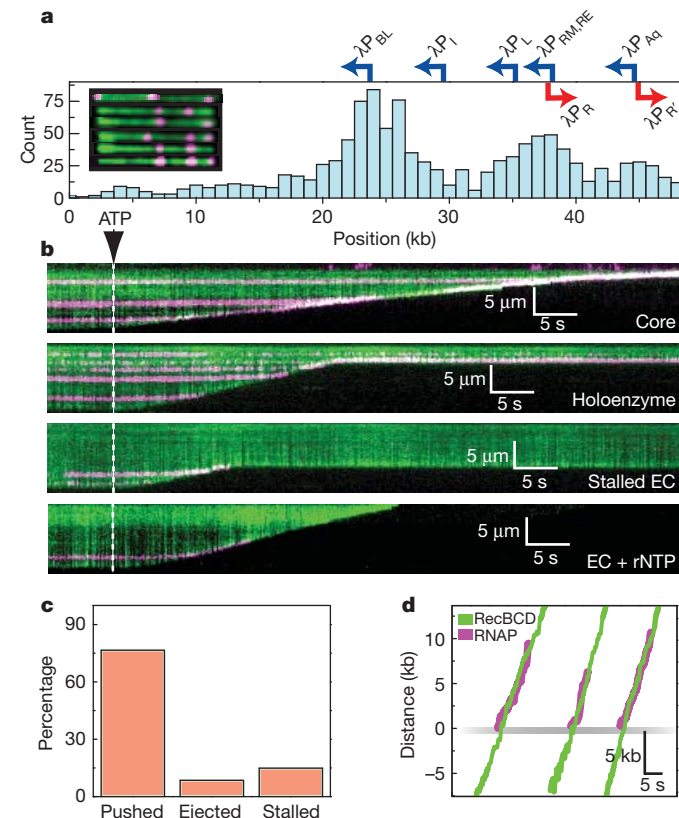


**Figure 1 | RecBCD removes RNAP from DNA.** **a**, Distribution of QD–RNAP bound to  $\lambda$  DNA. Locations of promoters are indicated; those facing left are shown in blue, those facing right are shown in red. The inset shows examples of YOYO-1-stained  $\lambda$  DNA (green) bound by RNAP (magenta). The tethered end of the DNA is on the left, and the free end of the DNA is on the right. kb, kilobase. **b**, Kymograms of RecBCD colliding with RNAP core, holoenzyme, stalled elongation complex (EC), and stalled elongation complex chased with ribonucleoside triphosphate (rNTP). Gaps in magenta traces correspond to quantum dot blinking. In these and all subsequent kymograms, the tethered end of the DNA is at the top, the free end is at the bottom, and buffer flow is from top to bottom. **c**, Distribution of event types. **d**, Tracking data for collisions, with traces aligned at the collisions.

<sup>1</sup>Howard Hughes Medical Institute, Columbia University, New York, New York 10032, USA. <sup>2</sup>Department of Biochemistry and Molecular Biophysics, Columbia University, New York, New York 10032, USA.

holoenzyme was heparin resistant ( $t_{1/2} \gg 6.7$  min,  $N = 58$ ), confirming open complex formation (Supplementary Fig. 3c, d). Bulk assays verified that QD-RNAP produced transcripts (Supplementary Fig. 3e), and single-molecule assays revealed a transcription velocity of  $15.7 \pm 8.6$  bp s $^{-1}$  ( $N = 20$ , 25 °C, 250 μM of each ribonucleoside triphosphate; Supplementary Fig. 3f).

When RecBCD collided with RNAP, the polymerase was rapidly ejected from DNA ( $t_{1/2} = 2.4 \pm 0.13$  s; Fig. 1b). Remarkably, RNAP could be pushed long distances ( $10,460 \pm 7,690$  bp,  $N = 44$ ; Fig. 1 and Supplementary Fig. 4) and RecBCD could disrupt core RNAP, holoenzymes, stalled elongation complexes and active elongation complexes (Fig. 1b and Supplementary Fig. 5). Out of 47 collisions with QD-RNAP holoenzyme, 15% (7 of 47) immediately stalled RecBCD, 8.5% (4 of 47) resulted in dissociation of RNAP with no sliding, 76.5% (36 of 47) of RNAP was pushed and 71% of pushed molecules were eventually ejected (Fig. 1c). The population of RNAP molecules that was directly ejected from the DNA increased ~5-fold for stalled and active elongation complexes (Supplementary Fig. 5). RecBCD also pushed and evicted RNAP labelled with 40-nm fluorescent beads or Alexa Fluor 488, arguing against nonspecific interactions between RecBCD and the quantum dots (Supplementary Fig. 6a). RecBCD did not slow or pause on colliding with RNAP (Fig. 1d and Supplementary Fig. 4a), nor was there any reduction in processivity in comparison with naked DNA ( $29,000 \pm 15,500$  bp). Similar outcomes were observed before and after Chi (not shown), indicating that RecBCD could dislodge RNAP regardless of whether RecB or RecD was the lead motor. We could unambiguously assign the orientation of RNAP at  $\lambda P_{BL}$  (Fig. 1a and Supplementary Fig. 3f), and RecBCD dislodged RNAP bound at  $\lambda P_{BL}$  during collisions in either direction (Fig. 1b and Supplementary Fig. 7a). RecBCD also pushed and ejected RNAP bound at all other locations regardless of DNA orientation (Fig. 1b). RecBCD even dislodged RNAP at lower velocities ( $446 \pm 192$  bp s $^{-1}$ ,  $122 \pm 128$  bp s $^{-1}$  and  $78 \pm 27$  bp s $^{-1}$  at 100 μM, 25 μM and 15 μM ATP, respectively; see Supplementary Fig. 7 and below), indicating that proteins could be dislodged even under suboptimal translocation conditions. We conclude that RecBCD disrupts RNAP regardless of orientation, transcriptional status or translocation velocity.

We next asked whether RecBCD could dislodge other proteins. EcoRI<sup>E111Q</sup> is a catalytically inactive version of EcoRI, which has high affinity ( $K_d = 2.5$  fM) for cognate sites and even binds tightly to non-specific DNA<sup>17</sup> ( $K_d = 4.8$  pM). EcoRI<sup>E111Q</sup> can halt *E. coli* RNA polymerase<sup>18,19</sup>; T7 and SP6 RNA polymerases<sup>20</sup>; SV40 large T antigen; *E. coli* UvrD, DnaB and T4 Dda helicases; SV40 replication forks<sup>21</sup>; and *E. coli* replication forks<sup>4</sup>. EcoRI withstands up to ~20–40 pN (ref. 22), and EcoRI<sup>E111Q</sup> binds cognate sites ~3000-fold stronger than wild-type EcoRI<sup>17</sup> ( $K_d = 6.7$  pM); thus, we infer that the catalytic mutant can resist at least as much force as the wild-type protein. lac repressor (LacI) is representative of a large family of bacterial transcription factors that has served as a model for transcriptional regulation and protein-DNA interactions. LacI binds tightly to specific sites<sup>23</sup> ( $K_d = 10$  fM for a 21-bp symmetric operator) but binds weakly to non-specific DNA<sup>24</sup> ( $K_d \geq 1$  nM) and slides rapidly along non-specific DNA rather than remaining at fixed locations<sup>25,26</sup>. LacI also blocks RNAP and replication forks both *in vitro* and *in vivo*<sup>18</sup>, highlighting that it is a potent and physiologically relevant barrier to translocase progression.

We labelled EcoRI<sup>E111Q</sup> and LacI with quantum dots (Supplementary Information), and QD-EcoRI<sup>E111Q</sup> and QD-LacI bound to the correct locations on the DNA substrates, confirming that the tagged proteins retained normal DNA-binding activity (Fig. 2a and Supplementary Fig. 8). QD-LacI was rapidly released from DNA by isopropyl-β-D-thiogalactoside, as expected (Supplementary Fig. 9). When RecBCD collided with EcoRI<sup>E111Q</sup>, it pushed the proteins  $13,000 \pm 9,100$  bp ( $N = 70$ ) before ejecting them from the DNA (Fig. 2b, c). In contrast, LacI was immediately ejected, and was not pushed within our resolution limits (Fig. 2b–d). There was no change

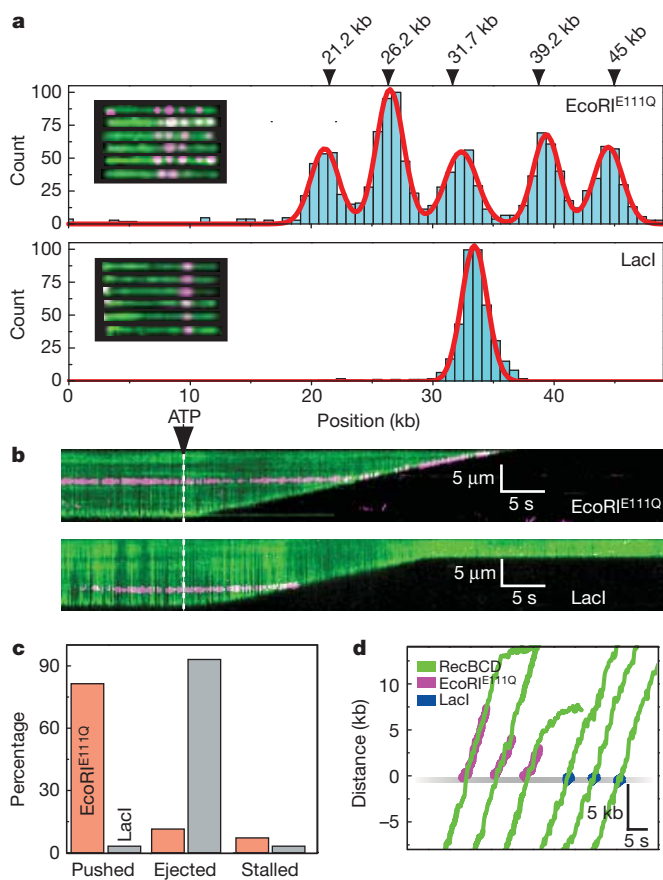


**Figure 2 | Disruption of EcoRI<sup>E111Q</sup> and lac repressor by RecBCD.**

a, Histogram of EcoRI<sup>E111Q</sup> (upper panel,  $N = 1,481$ ) and LacI (lower panel,  $N = 700$ ) bound to  $\lambda$  DNA. The locations of the five EcoRI sites found in  $\lambda$  DNA are indicated, along with examples of QD-EcoRI<sup>E111Q</sup> bound to YOYO-1-stained  $\lambda$  DNA (inset, upper panel) and examples of QD-LacI bound to the DNA (inset, lower panel). b, Kymograms showing RecBCD colliding with EcoRI<sup>E111Q</sup> and LacI (magenta), as indicated. d, Distribution of event types for EcoRI<sup>E111Q</sup> and LacI. e, Tracking data for individual collisions.

in velocity or processivity upon colliding with either protein (Fig. 2b, d and Supplementary Fig. 4). Out of 70 collisions with QD-EcoRI<sup>E111Q</sup>, 11.2% (5 of 70) stalled the translocase, 11.4% (8 of 70) resulted in immediate dissociation of EcoRI<sup>E111Q</sup> with no detectable sliding, 81.4% (57 of 70) of EcoRI<sup>E111Q</sup> was pushed along DNA and 92% of pushed molecules were eventually ejected (Fig. 2c). Out of 30 collisions with LacI, 3.3% (1 of 30) stalled the translocase, 93.3% (28 of 30) resulted in immediate dissociation of LacI with no detectable sliding and 3.3% (1 of 30) showed sliding before dissociation (Fig. 2c). A greater fraction of LacI might slide, but if so, the sliding events fall outside our resolution limits. Control experiments confirmed that RecBCD disrupted EcoRI<sup>E111Q</sup> labelled with fluorescent beads or Alexa Fluor 488 (Supplementary Fig. 6b). As with RNAP, RecBCD could strip EcoRI<sup>E111Q</sup> after Chi (not shown) and also disrupted EcoRI<sup>E111Q</sup> and LacI during low-velocity collisions (see below). These findings confirm that RecBCD readily displaces tightly bound proteins from DNA.

In eukaryotes, nucleosomes are the most frequently encountered DNA-bound obstacles. Replisomes, transcription machinery and ATP-dependent chromatin remodelers all act through mechanisms requiring force generation, and the response of nucleosomes to these forces remains a long-standing question in chromatin biology. Heterologous systems have revealed fundamental principles underlying these processes<sup>27,28</sup>: experiments with SP6 RNAP provided a theoretical framework for nucleosome repositioning<sup>27</sup>, and studies with phage T4 proteins were among the first to address the fate of nucleosomes during

replication<sup>28</sup>. Eukaryotic translocases exert forces in the same net direction as RecBCD, and RecBCD can unwind nucleosome-bound DNA<sup>29</sup>, arguing that it can serve as a good protein-based force probe for studying the fate of nucleosomes when rammed by a translocase.

Recombinant nucleosomes were deposited on DNA curtains by salt dialysis, as described<sup>9</sup>. Remarkably, RecBCD could push nucleosomes ( $7,311 \pm 5,373$  bp,  $N = 75$ ; Fig. 3), and similar results were obtained with fluorescently labelled H2A–H2B dimer or H3–H4 tetramer (Fig. 3a). Control experiments demonstrated that RecBCD could also push nucleosomes labelled with either fluorescent beads or Alexa Fluor 488 (Supplementary Fig. 6c). Out of 357 collisions with nucleosomes, 24% (84 of 357) immediately stalled RecBCD, 11% (40 of 357) resulted in direct nucleosome ejection, 65% (233 of 357) led to sliding (Fig. 3b) and ~50% of these were eventually ejected ( $t_{1/2} = 3.93 \pm 0.21$  s; Fig. 3b and Supplementary Fig. 4c). Nucleosomes reduced the processivity of RecBCD to  $14,000 \pm 7,000$  bp, as anticipated<sup>29</sup>, and the translocase stalled in a larger fraction of these collisions (24%) than in collisions with RNAP (15%), EcoRI<sup>E111Q</sup> (7%) and LacI (3.3%). Relative to the other roadblock proteins, fewer of the pushed nucleosomes (50%) were subsequently ejected from the DNA, and there was a 10% reduction ( $t$ -test,  $P = 0.00005$ ) in velocity while pushing nucleosomes (Fig. 3c and Supplementary Fig. 4c). These results demonstrate that intact nucleosomes can be pushed along DNA as theoretically predicted<sup>30</sup>, but indicated that RecBCD had more difficulty pushing and evicting nucleosomes than it did the other protein roadblocks. The finding that RecBCD pushes and evicts nucleosomes also rules out mechanisms requiring species-specific protein–protein interactions.

Protein disruption mechanisms can be described by at least four models, which differ in the nature of the mobile intermediates and the stage of the chemomechanical cycle during which the proteins dissociate (Fig. 4a). In the first model, passive release, the proteins (S) are dislodged from a high-affinity specific site and then pushed from one sequential nonspecific site to the next. Subsequent dissociation occurs spontaneously simply because the proteins are bound to lower-affinity nonspecific DNA (N). This model assumes that the proteins have similar low affinities for all nonspecific sites sampled, and predicts that the observed rates of RecBCD-induced dissociation ( $k_{\text{off,obs}}$ ) would be similar to that of spontaneous dissociation from nonspecific DNA in the absence of RecBCD ( $k_{\text{off,obs}} \approx k_{\text{off,N}}$ ). This model also predicts that the distance ( $d$ ) over which proteins are pushed will be proportional to velocity ( $V$ ) such that faster translocation will lead to longer distances and slower

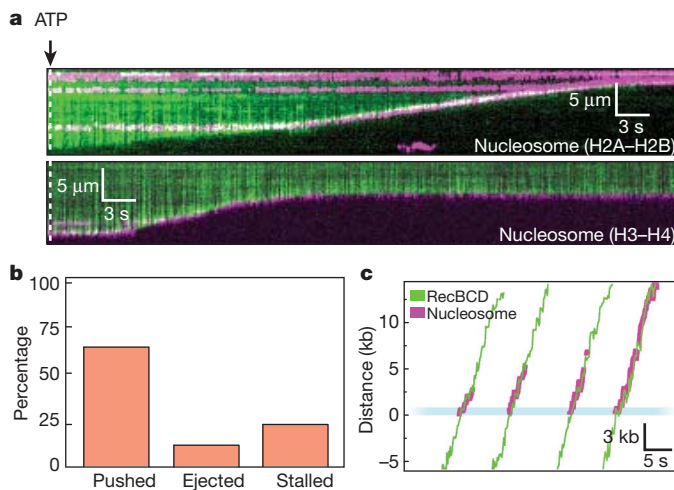


**Figure 3 | Nucleosomes can be pushed along DNA.** a, Kymograms showing RecBCD collisions with nucleosomes (magenta) that are labelled on either the H2A–H2B dimer or the H3–H4 tetramer, as indicated. b, Distribution of event types. c, Tracking data illustrating collisions between RecBCD and nucleosomes.

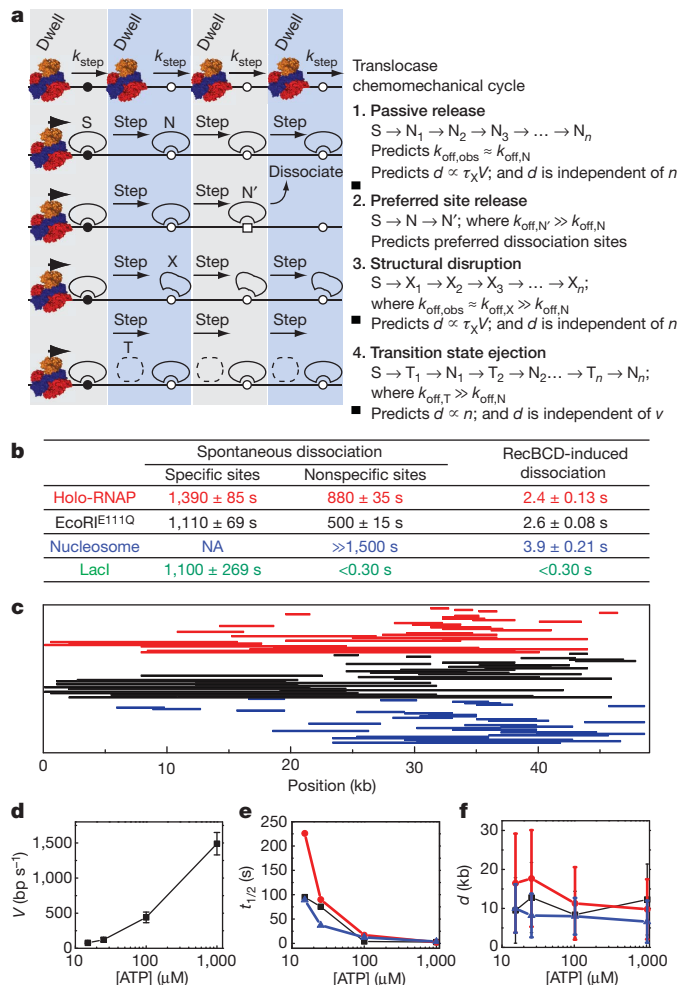


**Figure 4 | Protein displacement mechanisms.** a, Models for protein displacement (see main text). b, Spontaneous dissociation versus RecBCD-induced dissociation as determined from single exponential fits to dissociation data  $\pm$  s.d. Values for LacI nonspecific and RecBCD-induced dissociation represent upper bounds. Data are colour-coded for each different protein, as indicated. c, Representative sliding trajectories. Each line corresponds to the collision (right end point) and dissociation (left end point) for single proteins. d, RecBCD velocity (mean  $\pm$  s.d.) at different ATP concentrations ([ATP]). e, Protein  $t_{1/2}$  at different [ATP] values. Error was  $\leq 5.6\%$  of the reported values. f, Pushing distances (mean  $\pm$  s.e.m.) at different [ATP] values.

translocation will yield shorter distances. The second model, preferred site release, accounts for a situation in which proteins encounter rare sequences of exceptionally low affinity ( $N'$ ), such that they preferentially dissociate from these sites ( $k_{\text{off},N'} \gg k_{\text{off},N}$ ). In the third model, structural disruption, translocase collisions alter the conformation of the proteins (for example by permanently rupturing a subset of protein–DNA contacts) such that they persist as structurally perturbed complexes (X) after displacement from the high-affinity site. In this case, the mobile intermediates have a characteristic lifetime ( $\tau_X$ ) dictated by their weakened affinity for DNA, and this lifetime should be insensitive to translocation velocity. Therefore, the distance ( $d$ ) over which proteins are pushed will be proportional to velocity ( $V$ ), and faster translocation will lead to longer distances whereas slower translocation will yield shorter distances. The most important feature of this model, which distinguishes it from all of the other models, is that the structurally disrupted proteins are more weakly bound to DNA specifically as a consequence of the collision, such that the observed rate of RecBCD-induced dissociation ( $k_{\text{off,obs}}$ ) would be greater than the rate of spontaneous dissociation from nonspecific DNA ( $k_{\text{off,obs}} \approx k_{\text{off,X}} \gg k_{\text{off,N}}$ ). The fourth model, transition state ejection, is characterized by a series of

tightly bound nonspecific complexes (N) that must pass through a weakly bound transition state (T) as they are pushed from one position to the next. This model predicts that dissociation occurs predominantly during the transition state ( $k_{off,T} \gg k_{off,N}$ ). The time required to pass through the transition state during one round of the chemomechanical cycle is equivalent to the time required for the translocase to take a single step ( $k_{step}$ ), which is a fixed intrinsic value independent of ATP concentration. This relationship can be rationalized by considering that the velocity of RecBCD can be controlled by modulating ATP concentration (see below), with slower velocities resulting from longer dwell times between steps (while awaiting new ATP) rather than from changes in  $k_{step}$ . Therefore, the time it takes the roadblock to pass through the transition state during a single step will be independent of ATP concentration, whereas the cumulative time spent in the transition state will increase linearly with step number ( $n$ ) irrespective of the overall observed translocation velocity. The probability of dissociation will then increase with step number, the observed lifetimes will be inversely proportional to velocity and the total distance the proteins are pushed before dissociation will be independent of velocity (that is, the roadblocks will be pushed similar distances regardless of how fast the translocase moves).

Each aforementioned model makes distinct predictions that can be experimentally evaluated. This evaluation is easier for RNAP, EcoRI<sup>E111Q</sup> and nucleosomes because these proteins are pushed long distances (LacI is considered separately below). We first measured dissociation of these proteins from specific and nonspecific sites in the absence of RecBCD (Supplementary Information), and compared these results to RecBCD-induced rates of dissociation (Fig. 4b). RNAP, EcoRI<sup>E111Q</sup> and nucleosomes all bind tightly to nonspecific DNA, and RecBCD-induced dissociation was  $\geq 200$ -fold faster than spontaneous dissociation from nonspecific sites, which is inconsistent with passive release. We next analysed pushing trajectories to determine whether there was any evidence supporting preferred site release. Comparison of these trajectories revealed that RecBCD-induced dissociation of all three roadblock proteins occurred at random locations (Fig. 4c), arguing against preferred site release. To distinguish between structural disruption and transition state eviction, we compared protein lifetimes and pushing distances at four different translocation velocities (Fig. 4d). Remarkably, a 3.3-fold decrease in RecBCD velocity ( $446 \pm 192 \text{ bp s}^{-1}$  at  $100 \mu\text{M}$  ATP) led to 1.5-, 7.0- and 3.4-fold increases in the post-collision half-lives of EcoRI<sup>E111Q</sup>, RNAP and nucleosomes (Fig. 4e), respectively, although the distribution of distances over which the proteins were pushed remained largely unaltered (Fig. 4f and Supplementary Table 1). This effect was even more obvious at  $15 \mu\text{M}$  ATP, where a 19-fold decrease in RecBCD velocity ( $78 \pm 27 \text{ bp s}^{-1}$ ) led to 36-, 93- and 24-fold increases in the post-collision half-lives of EcoRI<sup>E111Q</sup>, RNAP and nucleosomes, respectively, but pushing distances were either unaltered or increased in comparison with those corresponding to the faster velocities. These results indicated that dissociation was dictated by the number of steps the proteins were forced to take rather than the cumulative time it took to be pushed a given distance, which is most consistent with transition state ejection. Although our experiments did not reveal any evidence for a structural disruption eviction mechanism, this does not rule out the possibility that EcoRI<sup>E111Q</sup>, RNAP and nucleosomes are structurally altered when acted upon by RecBCD. However, if they are structurally perturbed, this alone does not result in their eventual dissociation from DNA.

LacI differs from the other roadblocks in that it was immediately evicted from DNA, and the RecBCD-induced dissociation rate was comparable to the rate of spontaneous dissociation from nonspecific sites (Fig. 4b), which would seem consistent with a passive-release model. However, with current resolution limits we cannot completely rule out other mechanisms, and future studies will be necessary to fully address this issue. Importantly, RNAP, EcoRI<sup>E111Q</sup> and nucleosomes all bind tightly to nonspecific DNA, whereas LacI binds much more weakly to nonspecific sequences (Fig. 4b), suggesting that LacI is released more

rapidly from DNA after the collisions due to its weaker affinity for nonspecific sites. This result demonstrates that the roadblock proteins and the nature of their interactions with nonspecific DNA are critical contributing factors to the outcome of the collisions.

This leaves the question of how much force RecBCD exerts, and how much is sufficient to disrupt obstacles. Although our experiments do not yield a direct read-out of force, we can safely conclude that the force exerted by RecBCD is sufficient to displace RNAP, EcoRI<sup>E111Q</sup> LacI and nucleosomes from DNA. Our work has revealed unprecedented details of protein collisions on DNA and provides new insights into how translocases can disrupt nucleoprotein complexes. Given the flexibility of our experimental platform, we anticipate that these studies can be extended to other translocases and roadblock proteins, and it will be important to determine whether the mechanistic concepts developed here apply to different types of collision between proteins on DNA.

## METHODS SUMMARY

We conducted total-internal-reflection fluorescence microscopy experiments on a home-built microscope using nanofabricated DNA curtains, as previously described<sup>9</sup>. For all initial experiments, and for all kymograms shown in the manuscript, we used YOYO-1 to stain the DNA. YOYO-1 does not affect the translocation rate or processivity of RecBCD<sup>6</sup>, and it did not affect the binding distributions of RNAP, EcoRI<sup>E111Q</sup> or nucleosomes (not shown). In the presence of YOYO-1, the roadblock proteins showed the same general response to collisions with RecBCD, with identical distributions of ejection, stalling and pushing (and pushing velocities) seen with and without YOYO-1. However, the stain reduced the distance obstacles were pushed by 20–30%. Therefore, all sliding distances and half-lives reported here correspond to values measured in the absence of YOYO-1. Sliding distances are reported only for roadblock proteins that did not encounter any other quantum-dot-tagged proteins as they were pushed along the DNA. This ensures that each analysed collision/dissociation event involved only a single quantum-dot-tagged protein. Many reactions were observed in which multiple quantum-dot-tagged roadblock proteins were pushed into one another, but in these cases we could not determine the order in which each such protein was displaced from the DNA, and therefore could not measure sliding distances. To categorize the distributions of event type, we defined ‘sliding’ as the movement of any quantum-dot-tagged roadblock by more than  $0.53 \mu\text{m}$  ( $\sim 1,950 \text{ bp}$ ); anything less than this was scored as a direct dissociation event.

Received 8 August; accepted 6 October 2010.

Published online 24 November 2010.

- Jankowsky, E., Gross, C., Shuman, S. & Pyle, A. Active disruption of an RNA-protein interaction by a DExH/D RNA helicase. *Science* **291**, 121–125 (2001).
- Marquis, K. A. et al. SpollIE strips proteins off the DNA during chromosome translocation. *Genes Dev.* **22**, 1786–1795 (2008).
- Krejci, L. et al. DNA helicase Srs2 disrupts the Rad51 presynaptic filament. *Nature* **423**, 305–309 (2003).
- Guy, C. P. et al. Rep provides a second motor at the replisome to promote duplication of protein-bound DNA. *Mol. Cell* **36**, 654–666 (2009).
- Singleton, M. R., Dillingham, M., Gaudier, M., Kowalczykowski, S. & Wigley, D. Crystal structure of RecBCD enzyme reveals a machine for processing DNA breaks. *Nature* **432**, 187–193 (2004).
- Bianco, P. R. et al. Processive translocation and DNA unwinding by individual RecBCD enzyme molecules. *Nature* **409**, 374–378 (2001).
- Spies, M., Amitani, I., Baskin, R. & Kowalczykowski, S. RecBCD enzyme switches lead motor subunits in response to chi recognition. *Cell* **131**, 694–705 (2007).
- Taylor, A. F. & Smith, G. R. RecBCD enzyme is a DNA helicase with fast and slow motors of opposite polarity. *Nature* **423**, 889–893 (2003).
- Visnapuu, M.-L. & Greene, E. Single-molecule imaging of DNA curtains reveals intrinsic energy landscapes for nucleosome deposition. *Nature Struct. Mol. Biol.* **16**, 1056–1062 (2009).
- Ishihama, A. Functional modulation of *Escherichia coli* RNA polymerase. *Annu. Rev. Microbiol.* **54**, 499–518 (2000).
- Herbert, K. M., Greenleaf, W. J. & Block, S. M. Single-molecule studies of RNA polymerase: motoring along. *Annu. Rev. Biochem.* **77**, 149–176 (2008).
- Liu, B., Wong, M. & Alberts, B. A transcribing RNA polymerase molecule survives DNA replication without aborting its growing RNA chain. *Proc. Natl. Acad. Sci. USA* **91**, 10660–10664 (1994).
- Liu, B., Wong, M., Tinker, R., Geiduschek, E. & Alberts, B. The DNA replication fork can pass RNA polymerase without displacing the nascent transcript. *Nature* **366**, 33–39 (1993).
- Liu, B. & Alberts, B. Head-on collision between a DNA replication apparatus and RNA polymerase transcription complex. *Science* **267**, 1131–1137 (1995).

15. Pomerantz, R. T. & O'Donnell, M. The replisome uses mRNA as a primer after colliding with RNA polymerase. *Nature* **456**, 762–766 (2008).
16. Pomerantz, R. T. & O'Donnell, M. Direct restart of a replication fork stalled by a head-on RNA polymerase. *Science* **327**, 590–592 (2010).
17. Wright, D. J., King, K. & Modrich, P. The negative charge of Glu-111 is required to activate the cleavage center of EcoRI endonuclease. *J. Biol. Chem.* **264**, 11816–11821 (1989).
18. Epshtain, V. & Toulm, E. F. Rahmouni, A. Borukhov, S. & Nudler, E. Transcription through the roadblocks: the role of RNA polymerase cooperation. *EMBO J.* **22**, 4719–4727 (2003).
19. Nudler, E., Kashlev, M., Nikiforov, V. & Goldfarb, A. Coupling between transcription termination and RNA polymerase inchworming. *Cell* **81**, 351–357 (1995).
20. Pavco, P. A. & Steege, D. A. Characterization of elongating T7 and SP6 RNA polymerases and their response to a roadblock generated by a site-specific DNA binding protein. *Nucleic Acids Res.* **19**, 4639–4646 (1991).
21. Byrd, A. K. & Raney, K. D. Displacement of a DNA binding protein by Dda helicase. *Nucleic Acids Res.* **34**, 3020–3029 (2006).
22. Noom, M. C., van den Broek, B., van Mameren, J. & Wuite, G. J. L. Visualizing single DNA-bound proteins using DNA as a scanning probe. *Nature Methods* **4**, 1031–1036 (2007).
23. Sadler, J. R., Sasmor, H. & Betz, J. L. A perfectly symmetric lac operator binds the lac repressor very tightly. *Proc. Natl Acad. Sci. USA* **80**, 6785–6789 (1983).
24. Lin, S.-Y. & Riggs, A. D. Lac repressor binding to DNA not containing the lac operator and to synthetic poly DAT. *Nature* **228**, 1184–1186 (1970).
25. Elf, J., Li, G.-W. & Xie, X. Probing transcription factor dynamics at the single-molecule level in a living cell. *Science* **316**, 1191–1194 (2007).
26. Wang, Y. M., Austin, R. H. & Cox, E. C. Single molecule measurements of repressor protein 1D diffusion on DNA. *Phys. Rev. Lett.* **97**, 048302 (2006).
27. Studitsky, V. M., Clark, D. J. & Felsenfeld, G. Overcoming a nucleosomal barrier to transcription. *Cell* **83**, 19–27 (1995).
28. Bonne-Andrea, C., Wong, M. & Alberts, B. *In vitro* replication through nucleosomes without histone displacement. *Nature* **343**, 719–726 (1990).
29. Eggleston, A. K., O'Neill, T. E., Bradbury, E. M. & Kowalczykowski, S. C. Unwinding of nucleosomal DNA by a DNA helicase. *J. Biol. Chem.* **270**, 2024–2031 (1995).
30. Mollazadeh-Beidokhti, L., Deseigne, J., Lacoste, D., Mohammad-Rafiee, F. & Schiessl, H. Stochastic model for nucleosome sliding under an external force. *Phys. Rev. E* **79**, 031922 (2009).

**Supplementary Information** is linked to the online version of the paper at [www.nature.com/nature](http://www.nature.com/nature).

**Acknowledgements** We thank M. Gottesman, R. Gonzalez and members of the Greene laboratory for discussion and assistance throughout this work. We thank P. Modrich for providing an expression construct encoding EcoRI<sup>E111Q</sup>, R. Landick and K. Adelman for providing RNAP constructs, and J. Gelles for providing plasmids encoding RecBCD. I.J.F. was supported by an NIH Fellowship (F32GM80864). Funding was provided by the National Institutes of Health (GM074739 and GM082848 to E.C.G.). This work was partially supported by the Initiatives in Science and Engineering program through Columbia University, the Nanoscale Science and Engineering Initiative of the National Science Foundation under NSF Award Number CHE-0641523, and by the New York State Office of Science, Technology, and Academic Research. E.C.G. is an Early Career Scientist with the Howard Hughes Medical Institute. We apologize to colleagues whose work we were unable to cite owing to length restrictions.

**Author Contributions** I.J.F. did all cloning and ensemble-level biochemical characterization, and conducted and analysed RecBCD collision experiments with RNAP, EcoRI<sup>E111Q</sup> and LacI. M.-L.V. conducted and analysed RecBCD collision experiments with nucleosomes. I.J.F., M.-L.V. and E.C.G. discussed the data and co-wrote the paper.

**Author Information** Reprints and permissions information is available at [www.nature.com/reprints](http://www.nature.com/reprints). The authors declare no competing financial interests. Readers are welcome to comment on the online version of this article at [www.nature.com/nature](http://www.nature.com/nature). Correspondence and requests for materials should be addressed to E.C.G. (ecg2108@columbia.edu).